The International Journal of Advanced Manufacturing Technology (2019) 105:2523–2530
https://doi.org/10.1007/s00170-019-04385-8

ORIGINAL ARTICLE

First demonstration of a new additive manufacturing process based on metal extrusion and solid-state bonding

Jørgen Blindheim[1] · Torgeir Welo[1] · Martin Steinert[1]

Received: 10 March 2019 / Accepted: 2 September 2019 / Published online: 1 November 2019

Abstract
In this paper, a new additive manufacturing (AM) process based on extrusion and solid-state bonding is presented. The process uses metal feedstock wire which is processed in a continuous rotary extruder in order to disperse the surface oxides of the feedstock and to provide the required bonding pressure. Simultaneously, the die outlet is scraping the contact surface to provide an oxide-free interface between the extrudate and the substrate. Optical analyses of samples from a layered structure produced from AA6082 reveal that the stringers are fully merged; however, some voids and cracks are observed between the individual stringers. Still, this initial demonstration indicates that the process, upon further development, has high potential of producing near-net-shape parts at high deposition rates.

Keywords Additive manufacturing · Solid-state bonding · Continuous rotary extrusion

1 Introduction

During the last years, we have seen an increase in the industrial use of additive manufacturing (AM) technologies, opening for mass customisation of net-shape or near-net-shape parts that can potentially lead to less labour time, as well as reduced energy consumption and material waste compared to traditional subtractive processes. Additive processes can also provide increased design freedom as well as weight savings not achievable by traditional manufacturing processes.

AM of metals can be divided into three main categories regarding processing: powder bed fusion (PBF), directed energy deposition (DED) and sheet lamination (SL) [1]. In PBF, the part being produced is supported by the unconsolidated powder, thus providing great design freedom and the possibility to create detailed and complex shapes that are otherwise impossible to manufacture. However, the deposition rates for these processes are low, and the part size is limited by the powder bed size. For both the DED and SL categories, one finds processes covering the whole range from small or complex net-shape parts to the larger near-net-shape components at higher deposition rates. In the lower end of this range, one finds processes like droplet-based 3D printing [2, 3] and Acoustoplastic metal write [4], whereas wire arc additive manufacturing (WAAM) [5] and ultrasonic AM [6] are examples of high deposition rate processes for the DED and SL categories, respectively.

1.1 Melted-state AM processes for aluminium

For melted-state AM, the use of aluminium has been limited to a few alloys due to the resulting "as-cast" microstructure inherited from the melting. Only recently, it has been demonstrated that this problem can be overcome by the addition of nanoparticles acting as nucleation sites for new grains during PBF processing of AA7075 and AA6061, resulting in material strengths comparable with wrought material [7].

Still, most melted-state processes suffer from restrictions in the deposition rate due to limitations in the melt pool size. In addition, the contractions occurring during solidification and subsequent cooling usually lead to build-up of residual stresses in the structure, causing undesirable local and global deformations. Various mitigating actions have been undertaken to avoid such thermally induced distortions, like symmetric building, back-to-back building and the use of high-pressure inter-pass rolling [5]. WAAM based

✉ Jørgen Blindheim
jorgen.blindheim@ntnu.no

[1] Department of Mechanical and Industrial Engineering, Norwegian University of Science and Technology, NTNU, 7491, Trondheim, Norway

on the cold metal transfer (CMT) welding process has the capability to achieve high deposition rates, yet with increased material waste, since higher deposition rates contribute to a wider melt pool size and thus a thicker wall structure. A typical CMT deposition rate for aluminium, when keeping the buy-to-fly (BTF) ratio at 1.5, is 1 kg/h [5].

1.2 Solid-state AM processes for aluminium

AM processes based on friction joining were first patented in 2002 [8] and have later been commercialised for ultrasonic consolidation of thin sheets or foils [6]. Commercial ultrasonic machines from Fabrisonic are capable of depositing up to 1.3 kg/h. In recent years, a solid-state process based on friction welding has been developed, where the material is deposited onto the substrate using a rotating consumable rod [9]. Also, a process based on friction stir welding (FSW) has been demonstrated for bonding of stacked metal plates [10]. More recently, Aeroprobe has developed a modified FSW process, called MELD, where the feedstock is added through a rotating stirring tool [11].

Unlike melted-state processes, where the substrate is required to continuously solidify to keep its shape, solid-state processes have no such limitations in the deposition rate, as long as the deposition temperature is kept below the melting temperature of the material. This makes solid-state processes attractive for manufacturing of larger structures.

The overall aim of this research is to add knowledge to the field of solid-state AM, as a basis for development of new technology that enables deposition of the aluminium alloys commonly used in the automotive and aerospace industry today. The scope of this research covers a proof-of-concept demonstration of a new AM process based on continuous rotary extrusion and solid-state bonding.

In order for new manufacturing technology to be attractive to the industry, it needs to provide increased value as compared with commercially available manufacturing methods. For near-net-shape AM processes, when compared with subtractive methods, added value can be attributed to e.g. the ability to replace complex assemblies by a single part, reduced material waste or the possibility of producing functionally graded components. Therefore, in order to investigate the capabilities of this new process relative to more established AM processes, we use the following main performance parameters: (1) material properties, (2) deposition rates, (3) energy efficiency and (4) material efficiency.

Overall, the goals in this study are (1) to conduct a proof-of-concept test of an extruder and a deposition sequence and (2) to assess the technical feasibility and potentials of the proposed concept within the above-mentioned boundary conditions.

In Section 2, the operating principles of the proposed AM process are presented. Section 3 describes the experimental setup, while Section 4 presents the results and discusses the outcome based on the goals of this study. Finally, conclusions are given in Section 5.

2 Process description

The new process presented in this paper has emerged from the hybrid metal extrusion and bonding (HYB) technology, which originally was developed for joining of aluminium plates and profiles [12, 13]. The use of filler material addition during HYB welding may have some obvious advantages if adapted for AM purposes, which have sparked our interest in exploring the potential of such a process. The initial exploration and conceptualisation prior to this work are presented in previous studies [14, 15].

2.1 Bonding mechanisms

Historically, solid-state bonding was one of the first techniques used to bond two pieces of metal. Already in the middle bronze age, this technique was used for hammering smaller nuggets of gold to form larger pieces [16]. The first scientific study of cold welding was inspired by the Swedish scientist Mårten Triewald and published in 1724 by Desaguliers [17]. He describes how to bond two lead balls by cutting away a segment of each and pressing them together with a little twist. However, it was not until the middle of the twentieth century that the research was intensified, ultimately leading to a deeper understanding of processes like cold pressure welding, friction welding, accumulative roll bonding and extrusion of hollow sections.

The film theory was described by Bay in 1983 [18] and is still the way the bonding mechanisms are understood today. To achieve solid-state bonding, the virgin metal surfaces must be brought so closely together that metallic bonding occurs. For reactive materials like aluminium, however, the oxide layer either has to be removed prior to mating the bonding surfaces. Alternatively, the surfaces have to be expanded or deformed such that the oxide layer is cracked to allow the virgin materials to contact during deformation. An example of the former category is cold pressure welding, where oxides are removed through an outward material flow during compression [16]. Bonding through surface expansion, on the other hand, is utilised in processes like cold roll bonding and accumulative cold roll bonding [19].

Similar bonding mechanisms can also be observed in longitudinal seam welds of porthole die extrusions, where welds are formed under high pressure as the different material streams merge after flowing around the die bridges or webs [20–23]. The bonding mechanisms of these welds

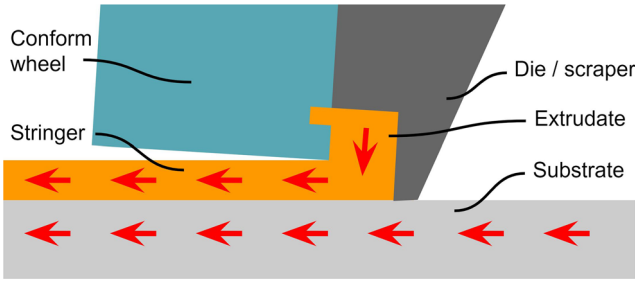

Fig. 1 Bonding is achieved as the metal streams of the oxide dispersed extrudate and the scraped substrate merges under high pressure

can be understood in both the above-mentioned ways, depending on whether a gas pocket is formed behind the bridge during extrusion causing oxides to form on the bonding interfaces, as pointed out by Yu et al. [23].

The metal flow in the new process proposed in this work resembles the one occurring during porthole die extrusion. However, in this case, the merging metal streams should be considered mating streams of extrudate and substrate, as illustrated in Fig. 1.

2.2 Extrusion principle

Continuous rotary extrusion, also known as conform extrusion [24, 25], serves two purposes in this process: First, when the feedstock is deformed in the extruder, oxides present on the feedstock surface are dispersed into the extrudate. Secondly, the extruder provides the required pressure to obtain bonding at the interface between the extrudate and the substrate. Following the illustration in Fig. 2a, the feedstock wire is firmly pressed into the groove of a rotation wheel. The wheel is sealed by a housing provided with an abutment with a die at the end. The surface area of the grove is larger than the exposed surface of the housing, thus creating a net driving force in the direction of rotation. When the feedstock is blocked by the abutment,

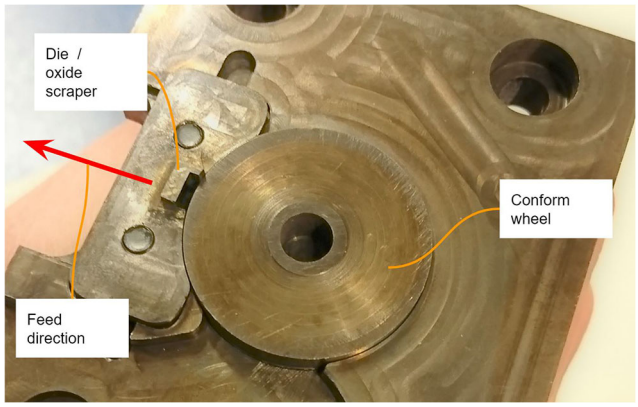

Fig. 3 The extruder head as seen from underneath

axial compression is induced, causing the material to fill the entire cross-section. This, in turn, increases the contact area and friction further and leads to a pressure build-up. When the required extrusion pressure is obtained, the material is extruded through the die outlet close to the abutment.

2.3 Deposition sequence

Figure 2b illustrates the deposition sequence applied in this study. A blank of aluminium is fixed in the machine, acting as a substrate upon which the first layer is bonded. The extruder adds material as it moves in the deposition direction, placing stringers side-by-side to form a layer, allowing new layers to be added. The die outlet is scraping both the underlying layer and the side wall of the adjacent stringer to remove the oxides and create favourable conditions for bonding with the extrudate. To ensure that the scraper touches the mating surfaces, 0.1 mm of the adjacent stringer and under-laying surface is cut away by the scraper within each pass.

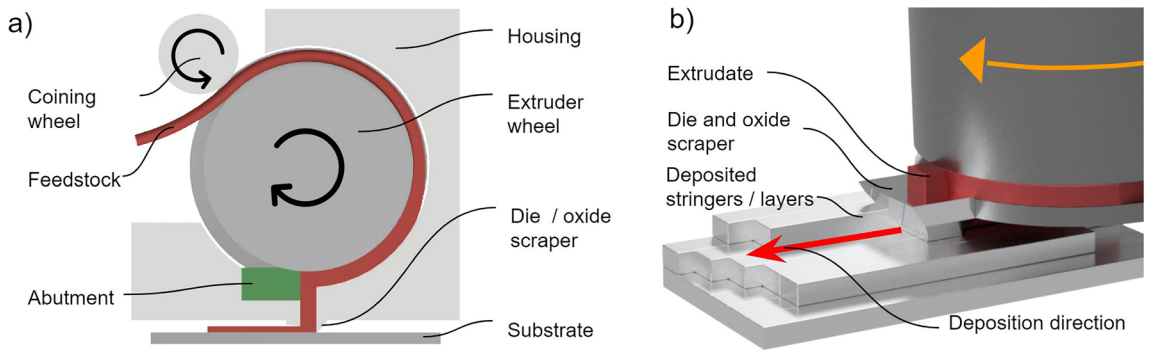

Fig. 2 Principal illustrations of the extruder. **a** The extruder consists of a slotted wheel running over a stationary housing. A coining wheel is used to firmly press the wire into the slot, causing the rotating wheel to grip the wire. The extrusion pressure is built up as the material is blocked by the abutment. The die also act as a scraper in order to remove oxides from the substrate prior to bonding with the extrudate. **b** The wheel and the die along with a deposited structure

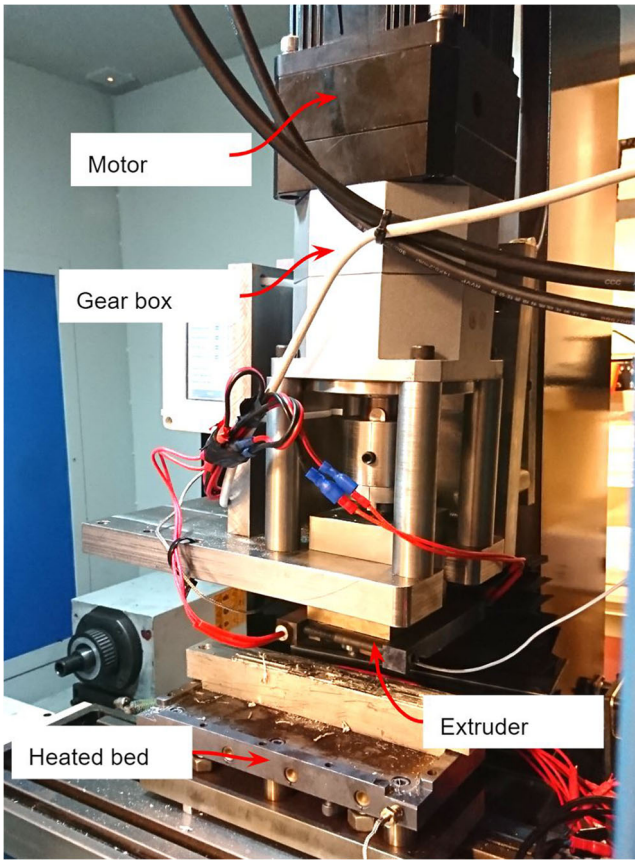

Fig. 4 The extruder attached to a CNC milling machine. A heated bed is used to control the temperature of the deposited structure

3 Experimental

3.1 Setup

A Sieg SX3 CNC milling machine was used to control the speed and position of the extruder during deposition. The extruder wheel, house and the die of the extruder (Fig. 3) were produced from hardened Uddeholm Orvar Supreme tool steel. The extruder is driven by a 1.8 kW servo motor connected through a gearbox with a gear reduction of 30. Torque data was measured through a Smowo LCS-T5 torque cell and a HX711 ADC, wirelessly connected to a computer. Nichrome heat cartridges and a *K*-type thermocouple were inserted into the print bed and used to control the substrate temperature during deposition from a PID controller. The extruder house was, by the same means, pre-heated to soften and increase the formability of the feedstock material prior to extrusion. The experimental setup is depicted in Fig. 4 and some key data for the extruder is listed in Table 1.

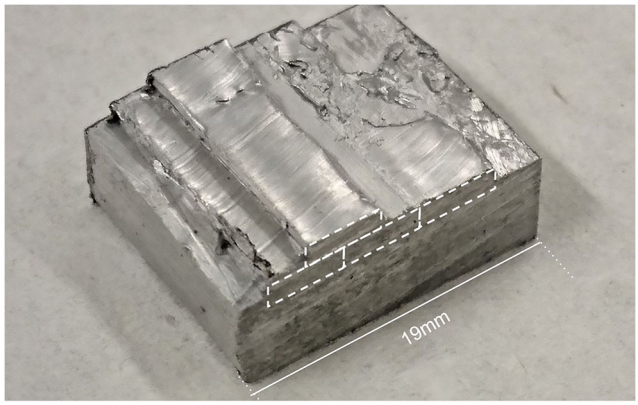

Fig. 5 Photograph of a deposited sample of AA6082

3.2 Process parameters

Figure 5 shows a two-layered structure deposited by this process. The operational conditions are summarised in Table 2. The feedstock material was a 1.6 mm AA6082 wire in T4 temper, deposited to a cross-section of 0.9 mm × 4 mm onto a substrate of the same alloy. Table 3 gives the chemical composition of the AA6082 feedstock material.

3.3 Sample preparation

Samples used for macrostructural analyses were prepared according to standard preparation procedures. To reveal the macrostructure of the bonding interfaces, the specimens were immersed in a 1% sodium hydroxide solution for 10 min. The macrographs of the samples were captured using an Olympus BX35M light microscope and an Alicona confocal microscope.

Table 1 Specifications for the extruder

Parameter	Value
Wire diameter	1.6 mm
Max speed	100 RPM
Max deposition rate	2150 g/h
Outlet dimensions (w × h)	4 mm × 1 mm
Extruder wheel outer diameter	28 mm

Table 2 Parameters used in the experimental setup

Parameter	Value
Pin rotation speed	4.3 RPM
Feed rate	200 mm/min
Deposition rate	116 g/h
Applied torque	175 Nm
Deposition temperature	450 °C

Table 3 Chemical compositions of AA6082 feedstock material

Fe	Si	Zn	Mn	Mg	Cu	Ti	Al (balance)
< 0.50	0.7–1.3	< 0.2	0.4–1.0	0.6–1.2	< 0.1	< 0.1	95.2–98.3

4 Results and discussion

4.1 Interpretation of governing mechanisms

The sample depicted in Fig. 5 has been sectioned for observation of the bonding interfaces between the individual stringers. Optical macrographs are shown in Fig. 6.

Figure 6a shows the substrate material with two layers deposited on top. From the macrograph, it is visible how the stringers have been conformed to the underlying material, indicating that the interfaces have been subjected to contact pressures above the flow stress of the material. Still, defects in the form of cracks can be observed between the individual stringers, as depicted in Fig. 6c, meaning that the layers are not fully bonded. A possible reason for this can be oxide formation on the interfaces during deposition. This failure mode is similar to that observed in longitudinal seam welds in porthole die extrusion, when a gas pocket is present behind the bridge [23]. In the case of the demonstrated process, the pressure at the bonding interface is controlled by the rotational speed and the scanning speed of the extruder. If the extruder moves too fast, it will not provide sufficient material flow to allow for pressure build-up in the die cavity, thus, forming a gas pocket.

Figure 6b displays a pore between the two stringers of the first layer. Higher extrusion pressure can to some extent prevent this defect. However, a more suitable solution is to reduce the angle of the sidewall of the adjacent stringer in order to avoid the sharp corner and thus create more favourable material flow conditions. Still, this proof-of-concept study has demonstrated that the extruder is capable of processing and depositing advanced aluminium alloys. More extensive laboratory testing is required to further investigate the governing mechanisms of this process and to determine the mechanical properties of the deposited material. Future work will focus on these aspects.

4.2 Deposition rates

From an industrial perspective, deposition rates are crucial for increasing the manufacturing efficiency. The deposition rate of the suggested process is controlled by the circumferential velocity of the conform wheel and the diameter of the feedstock wire. The current extruder design,

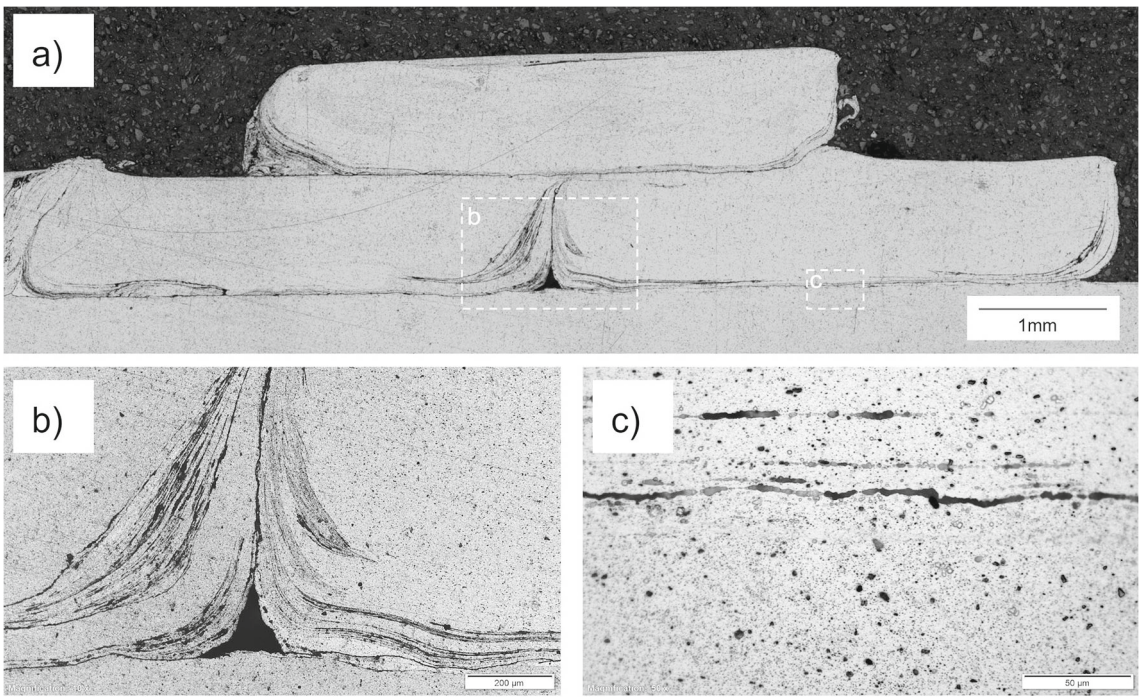

Fig. 6 Optical macrographs of **a** a transverse section of a deposited structure, **b** pore formation at the interface between two adjacent stringers, and **c** cracks on the interface between the substrate and a stringer

which uses Ø1.6 mm feedstock wire, yields a deposition rate of more than 2 kg/h at its maximum speed of 100 RPM. This high deposition rate makes this AM technology particularly suitable for manufacturing of larger structures where this capability can be fully utilised. In theory, the deposition rate is only limited by the scaling of the process. However, the deposition rate must be balanced and compatible with other requirements, such as the scanning speed, the die geometry, the process temperature and the contact pressure at the bonding interface. Future experiments will be carried out at higher deposition rates to investigate the optimal parameters for achieving proper bonding between the extrudate and the substrate.

4.3 Energy efficiency

The work done on the deposited material can be calculated from the rotational speed and the supplied torque on the extruder along with the feed distance and the applied force in the feed direction from the following formula:

$$W_i = 2\pi MN + Fs$$

Referring to Table 2, the extruder is subjected to a torque of M= 175 Nm at a rotational speed of N= 4.3 RPM and a feed speed of 200 mm/min. Assuming sticking friction over the contact area of the die outlet, the force in the feed direction, F, will be in the order of 1500 N at the extrusion temperature. The supplied power during the experimental run is calculated to be 84 W.

Furthermore, to calculate the energy efficiency of the process, the applied work should be compared with that of the required heat input to bring the material up to extrusion temperature. The latter can be estimated from the specific heat capacity of the feedstock material, c= 987 J/kgK, the deposition rate and the temperature change, $\Delta T = 430\ K$ from

$$Q_r = cm\Delta T$$

The overall efficiency of the process then becomes $\eta = 0.16$, conclusively demonstrating that the process generates excess heat which needs to be dissipated during processing. Still, when comparing against the CMT process, Dutra et al. reported a power consumption of 1430 W for welding of AA5183 Ø1.2 mm wire at 7 m/min [26]. Under the assumption of linearity between the power input and the deposition speed, the energy consumption of this new process is 30% less than that of the CMT process.

4.4 Materials

In this proof-of-concept study, the technology has been demonstrated for an Al-Mg-Si alloy commonly used for various structural applications. However, the process also has the potential of depositing other advanced aluminium alloys or extrudable metals. Joining the material in the solid state eliminates the defects associated with melting of the material and maintains the wrought properties of the material through processing. This opens for creating AM parts from a wider range of aluminium alloys, even from the more advanced aerospace 7000-series, which for most purposes are considered unweldable by the melted-state processes. Furthermore, the nature of additive processing means that the feedstock composition can be altered during processing to create functionally graded components having tailored material properties in specific regions of a part.

For precipitation hardening alloys, like Al-Mg-Si, it is necessary to carry out solution heat treatment followed by quenching and ageing to utilise the full-strength potential of the part. By depositing at the solution heat treatment temperature, the part can be soaked for the required time for supersaturation of the whole structure. Finally, after quenching, the desired ageing cycle can be carried out to control the formation of precipitates.

4.5 Material utilisation

The relatively coarse near-net-shape structure requires subtractive machining to obtain the final shape and tolerances. This final processing step will cause material waste depending on the requirements of the net-shape; however, obviously with significantly less waste than that of machining from solid blanks. Allen lists BTF ratios ranging from 6 to 20 for some typical titanium aeroengine components [27], while Barnes [28] reports a BTF industry average of 11 for machined parts. Martina and Williams [29] considered different manufacturing options for a 15 kg aluminium wing rib and calculated a cost reduction of 65% for producing it by the WAAM process at a deposition rate of 1 kg/h and a BTF ratio of 2.3, as opposed to 40 for machining from a solid blank. With the new process proposed in this paper, it is reasonable to achieve BTF ratios comparable with that achieved by the WAAM process, depending on the final part geometry.

4.6 Further developments

The further development of this AM process towards real-world industrial application will focus on optimisations with regard to extruder design and process control. From the proof-of-concept testing conducted herein, it was observed that material accumulation on the bottom of the extruder wheel is causing some process instability. An isolated die design, inhibiting the extruder wheel to interfere with the deposited material, has the potential to prevent this issue, but at the cost of increased extrusion pressure due to increased die length. Furthermore, the diameter of the

extruder wheel should be adapted to the required extrusion chamber length for the required extrusion pressure in order to reduce friction, and thus the required torque to rotate the extruder.

5 Conclusions

This paper has presented a new solid-state AM process based on continuous extrusion and bonding of metal feedstock wire. The main objectives of the investigation were to conduct a proof-of-concept demonstration of the process and assess its potentials. Through this preliminary investigations, the technical feasibility has been conclusively demonstrated by successfully depositing a near-net-shape structure of AA6082. The process operates below the melting temperature and has thus the potential of achieving high deposition rates. The fact that no material melting is involved, means that potential problems related to hot cracking and residual stresses are reduced compared with those associated with conventional melted-state processes. The energy efficiency of the process is higher or comparable with that of established AM processes.

Future work will focus on process optimisation, along with laboratory testing to determine mechanical properties and the bonding strength between the deposited stringer beads and the layers.

Acknowledgements The authors are thankful to Vidar Berg for providing a solution to transferring torque data from a rotating shaft. They are also indebted to Hybond AS and Øystein Grong for valuable assistance.

Funding information This work is financially supported by NTNU, NAPIC (NTNU Aluminium Product Innovation Center) and the KPN project Value sponsored by the Research Council of Norway, Hydro and Alcoa.

References

1. ASTM (2015) Standard terminology for additive manufacturing – general principles – terminology. ISO/ASTM 52900:2015(E)
2. Yi H, Qi L, Luo J, Zhang D, Li N (2019) Direct fabrication of metal tubes with high-quality inner surfaces via droplet deposition over soluble cores. J Mater Process Technol 264:145–154. https://doi.org/10.1016/j.jmatprotec.2018.09.004. https://linkinghub.elsevier.com/retrieve/pii/S0924013618303959
3. Yi H, Qi L, Luo J, Zhang D, Li H, Hou X (2018) Effect of the surface morphology of solidified droplet on remelting between neighboring aluminum droplets. Int J Mach Tools Manuf 130–131:1–11. https://doi.org/10.1016/j.ijmachtools.2018.03.006. https://linkinghub.elsevier.com/retrieve/pii/S089069551830066X
4. Deshpande A, Hsu K (2018) Acoustoplastic metal direct-write: Towards solid aluminum 3d printing in ambient conditions. Addit Manuf 19:73–80. https://doi.org/10.1016/j.addma.2017.11.006. https://linkinghub.elsevier.com/retrieve/pii/S2214860417300234
5. Williams SW, Martina F, Addison AC, Ding J, Pardal G, Colegrove P (2016) Wire + arc additive manufacturing. Mater Sci Technol 32(7):641–647. https://doi.org/10.1179/1743284715Y.0000000073
6. White DR (2003) Ultrasonic consolidation of aluminum tooling. Adv Mater Processes 161(1):64–65
7. Martin JH, Yahata BD, Hundley JM, Mayer JA, Schaedler TA, Pollock TM (2017) 3d printing of high-strength aluminium alloys. Nature 549(7672):365–369. https://doi.org/10.1038/nature23894
8. White D (2002) Object consolidation employing friction joining. US6457629
9. Dilip JJS, Rafi HK, Ram GJ (2011) A new additive manufacturing process based on friction deposition. Trans Indian Inst Metals 64(1–2):27
10. Palanivel S, Nelaturu P, Glass B, Mishra R (2015) Friction stir additive manufacturing for high structural performance through microstructural control in an Mg based WE43 alloy. Mater Des (1980-2015) 65:934–952. https://doi.org/10.1016/j.matdes.2014.09.082
11. Schultz J, Creehan K (2014) System for continuous feeding of filler material for friction stir welding, processing and fabrication
12. Grong Y (2012) Recent advances in solid-state joining of aluminum. Weld J 91(1):26–33
13. Sandnes L (2017) Preliminary benchmarking of the HYB (Hybrid metal extrusion & bonding) process for butt welding of AA6082-T6 plates against FSW and GMAW. Master's thesis, Norwegian University of Science and Technology
14. Blindheim J, Grong Y, Aakenes UR, Welo T, Steinert M (2018) Hybrid metal extrusion & bonding (HYB) - a new technology for solid-state additive manufacturing of aluminium components. Procedia Manufacturing 26:782–789. https://doi.org/10.1016/j.promfg.2018.07.092. https://linkinghub.elsevier.com/retrieve/pii/S2351978918307637
15. Blindheim J, Welo T, Steinert M (2019) Rapid prototyping and physical modelling in the development of a new additive manufacturing process for aluminium alloys. Procedia Manufacturing. https://doi.org/10.1016/j.promfg.2019.06.212
16. Tylecote R (1968) The solid phase welding of metals. The solid phase welding of metals, Edward Arnold
17. Desaguliers JT (1724) Some experiments concerning the cohesion of lead. Philos Trans R Soc Lond 33(389):345–347. https://doi.org/10.1098/rstl.1724.0065
18. Bay N (1983) Mechanisms producing metallic bonds in cold welding. WELDING J 62(5):137
19. Saito Y, Utsunomiya H, Tsuji N, Sakai T (1999) Novel ultra-high straining process for bulk materials—development of the accumulative roll-bonding (ARB) process. Acta materialia 47(2):579–583
20. Akeret R (1992) Extrusion welds-quality aspects are now center stage. In: Proceedings of the 5th International Aluminium Extrusion Technology Seminar, 1992
21. Valberg H (2002) Extrusion welding in aluminium extrusion. Int J Mater Prod Technol 17(7):497–556
22. Yu J, Zhao G (2018) Interfacial structure and bonding mechanism of weld seams during porthole die extrusion of aluminum alloy profiles. Mater Charact 138:56–66. https://doi.org/10.1016/j.matchar.2018.01.052
23. Yu J, Zhao G, Chen L (2016) Analysis of longitudinal weld seam defects and investigation of solid-state bonding criteria in porthole die extrusion process of

aluminum alloy profiles. J Mater Process Technol 237:31–47. https://doi.org/10.1016/j.jmatprotec.2016.05.024
24. Etherington C (1974) Conform - a new concept for the continuous extrusion forming of metals. J Eng Ind 96(3):893–900
25. Green D (1972) Continuous extrusion-forming of wire sections. J INST MET 100:295–300
26. Dutra JC, Gonçalves E, Silva RH, Marques C (2015) Melting and welding power characteristics of MIG–CMT versus conventional MIG for aluminium 5183. Weld Int 29(3):181–186. https://doi.org/10.1080/09507116.2014.932974. http://www.tandfonline.com/doi/abs/10.1080/09507116.2014.932974
27. Allen J (2006) An investigation into the comparative costs of additive manufacture vs. machine from solid for aero engine parts. In: RTO-MP-AVT-139, p 10
28. Barnes J, Kingsbury A, Bono E (2016) Does low cost titanium powder yield low cost titanium parts?
29. Martina F, Williams S (2015) Wire+arc additive manufacturing vs. traditional machining from solid: a cost comparison. Tech. rep